

UNIVERSIDADE DE SÃO PAULO  
Escola de Engenharia de São Carlos – EESC-USP  
DEPARTAMENTO DE ENGENHARIA AERONÁUTICA

ALBA GRAU MORESO

FLOW-BODY INTERACTION, SELF-INDUCED RESONANT VIBRATIONS  
BY VORTEX SHEDDING ON A BLADELESS WIND TURBINE OF  
MATERIALS WITH HIGH ELECTROMECHANICAL COUPLING

SUPERVISOR: PROF. HERNAN CERÓN MUÑOZ

SÃO CARLOS - SP  
2017

# Abstract

A theoretical analysis of the bladeless wind turbine, recently invented by Vortex Bladeless S.L., is presented. The aerodynamics and vibrations involved are studied, as well as the function of materials with high electromechanical coupling on this device.

The wind turbine studied works thanks to resonant vibrations self-excited by the vortex street developed downwash the structure. The aeroelastic energy absorbed is transformed into electrical energy due to the high electromechanical coupling of the materials the structure is built with.

The study begins with the initial vortex generation on the stationary case. The vortex street and the fluid forces on a cylinder are analysed and a simile of the device and the flow around tall buildings is made. The literature available about the Strouhal number on wind turbines is revised and the importance of the wind gradient in wind engineering is also observed.

Then the interaction between the vibration of a cylinder and the vortex street generated is studied. The vortices development changes and with that, the fluid forces over the structure too. We study the resonance effect and with it, the aeroelastic instability, flutter, which is the objective of the device in order to maximize the energy absorption.

To finish the process, the transformation of the mechanical energy from the oscillation into usable electrical energy is performed through the high electromechanical coupling of the materials of the structure. This function of the materials, and the modulation of the natural frequency of the structure by modifying the voltage input are analysed.

Finally, an introduction of the basis of a software (FSI) to perform computational analysis of fluid-structure interaction problems is presented, as these problems are shown in many engineering and architecture applications.

**Keywords:** bladeless wind turbine, vortex street, resonance, electromechanical coupling, wind gradient, Strouhal, flutter, fluid-structure interaction.

# List of Illustrations

Figure 1 - Vortex's prototype created by Vortex Bladeless.....	5
Figure 2 - Various types of flow over a circular cylinder. ....	8
Figure 3 - Strouhal number estimations by many authors for a variety of periodic fluid flows .....	11
Figure 4 - Computed time-averaged vorticity contour on the symmetrical plane in a shear flow around a tall building .....	12
Figure 5 - Instantaneous velocity vectors in a shear flow around a tall building during vortex- shedding process .....	12
Figure 6 - Wind gradient with different Hellmann's exponents.....	13
Figure 7 - Radius of the column depending on his height [1].....	14
Figure 8 - Vortex generation frequencies along the mast with 1) Variable section, 2) Constant section.....	14
Figure 9 - Lateral vibrations of a cylinder and wake regions formed.....	15
Figure 10 - Forced response of a spring-mass system driven harmonically at its natural frequency, called resonance[23].....	17
Figure 11 - Magnitude of the steady-state response versus the frequency ratio for several values of the damping ratio ( $\xi$ ) [23].....	17
Figure 12 - Examples of conforming mesh (a) and non-conforming mesh (b) .....	22

# Summary

Abstract.....	2
List of Illustrations .....	3
Summary .....	4
Introduction .....	5
1. Objectives.....	7
2. Theoretical Analysis.....	8
2.1. Aerodynamical analysis .....	8
2.1.1. Fixed structure .....	8
2.1.2. Vibrating structure .....	15
2.2. Resonance .....	17
2.3. Electromechanical coupling.....	19
3. Computational Analysis.....	20
3.1. FSI software.....	20
Conclusions.....	23
References.....	24

## Introduction

Procuring clean and renewables sources of energy, as a replacement for fossil fuels, has been a big global concern since approximately the 1970s. The research and investment on renewable energy has become significant, and it is increasing more and more with the years. Of all these sources of energy, wind power was in 2015 the second one on the list of global investment, after solar power, with an investment of 109 billion USD approximately.<sup>1</sup>

Thanks to all this research during decades, many types of devices have been created and improved for obtaining electrical power from the wind's kinetic energy. Nowadays, wind turbines are classified in two main groups, the most common ones rotate about a horizontal axis and the other ones about a vertical axis. There are big wind farms for commercial production and small devices for private use spread around the world. However, these two types of devices are essentially very similar. Wind's kinetic energy is transferred through the rotation of blades to an electrical generator and, with the movement of the rotor inside a magnetic field, electrical power is obtained.

The wind power scenario could change after the revolutionary wind turbine, Vortex, created by the Spanish company Vortex Bladeless, founded by David Suriol, David Yáñez and Raul Martín. The already patented and under development new wind turbine is bladeless, it consists on a big conical structure that takes advantage of wind's vorticity to vibrate (Figure 1).



*Figure 1 - Vortex's prototype created by Vortex Bladeless*

---

<sup>1</sup> For more renewable sources global data, see Renewables 2016 Global Status Report

Wind's vorticity could be very dangerous for structures like tall buildings or bridges, it can lead to an oscillating motion that could reach resonance and cause the collapse of the structure. While architects and engineers have been avoiding this effect, Vortex Bladeless's founders saw an opportunity, this enormous amount of energy could be used.

The general performance of Vortex is based on three physics fundamentals: the development of Von Karman vortices on a flow hitting a conical structure, resonance and materials with high electromechanical coupling. These three physical principles have never been combined before for electrical energy generation.

The process begins with an oscillation produced by wind's vorticity and the movement is helped by the attraction and repelling of two rings of magnets on the base of the cone. The movement of the structure enhances the vortex generation. The objective is to adjust the natural frequency of the structure to the vortex generation frequency, and this way, achieve resonance to maximize the aeroelastic energy absorption. As the structure is made of materials with high electromechanical coupling, the movement of the mast will produce a potential difference, and usable electrical energy will be obtained. [1]

The main structural differences of Vortex with the current wind turbines are: Vortex has no mobile parts, the generator is located at the bottom so the CG is located lower, the structure is an empty cone made of fiber glass, light and environmentally friendly. [2] This revolutionary wind turbine could end with some problems that current rotating wind turbines have. A comparison of Vortex and rotating wind turbines is showed below.

		✓ Pros	✗ Cons
<b>Rotating wind turbines</b>	HAWT	<ul style="list-style-type: none"> <li>✓ Very developed</li> <li>✓ 60 % efficiency</li> </ul>	<ul style="list-style-type: none"> <li>✗ Affects migration of birds</li> <li>✗ Noise</li> <li>✗ Low energetic density</li> <li>✗ Needs wind orientation</li> </ul>
	VAWT	<ul style="list-style-type: none"> <li>✓ No orientation needed</li> <li>✓ Lower noise</li> <li>✓ High energetic density</li> </ul>	<ul style="list-style-type: none"> <li>✗ Low efficiency</li> <li>✗ Need external power to start</li> <li>✗ Lower stability</li> <li>✗ Lower resistance to high velocity winds</li> </ul>
<b>Vortex</b>		<ul style="list-style-type: none"> <li>✓ 80% reduction of weight</li> <li>✓ 50% less material</li> <li>✓ Low noise</li> <li>✓ Does not affect bird migration</li> <li>✓ High energetic density</li> <li>✓ Less maintenance and oil waste (no mobile parts)</li> <li>✓ High range of velocity winds</li> <li>✓ No orientation needed</li> </ul>	<ul style="list-style-type: none"> <li>✗ 30 % lower production than HAWT</li> <li>✗ Bigger initial inversion</li> </ul>

Table 1 - Pros and cons of rotating wind turbines compared to Vortex [1]

# 1. Objectives

The main objective of this paper is to analyse theoretically the behaviour and energy transformation process of the revolutionary patented bladeless wind turbine “Vortex”, using the literature available.

Therefore, we will study the physical phenomena involved, such as aerodynamics and aeroelastic effects, vibrations and resonance phenomenon or the use of materials with high electromechanical coupling on the structure. Those are physical fundamentals that have never been used together before on a wind turbine

A detailed analysis of the whole process of wind’s energy transformation into usable electrical energy in “Vortex” is presented. Beginning with the stationary aerodynamics involved, we continue analysing the vibration of the structure and seeing how the vibration affects the surrounding flow and the vortex generation. After the aerodynamical analysis, a study of the resonance achieved by the structure is made as well as the aeroelastic effect produced, “flutter”. The study finishes with the last part of the process, the function of the materials with high electromechanical coupling in the transformation of mechanical energy into usable electrical energy.

Finally, we will introduce the basis of a useful software to perform computational analysis of fluid-structure interaction problems, FSI. These problems are complex to simulate and are still a challenge, but they are present on many engineering applications.

## 2. Theoretical Analysis

After the brief explanation of the device, we will analyse in detail the complete process of the "Vortex" wind turbine transformation of wind's energy on electrical energy, with help of the literature available.

We will divide the analysis on the three physics fundamentals explained before.

### 2.1. Aerodynamical analysis

#### 2.1.1. Fixed structure

The process begins with a laminar, stationary, viscous airflow colliding against the surface of the mast, producing eddies downwash. This flow is dominated by friction effects.

We could make a first approach, to study the aerodynamics, analysing the flow over a circular cylinder. [3]

Next figure shows the variation of the flow field around a circular cylinder, when increasing the Reynolds number.

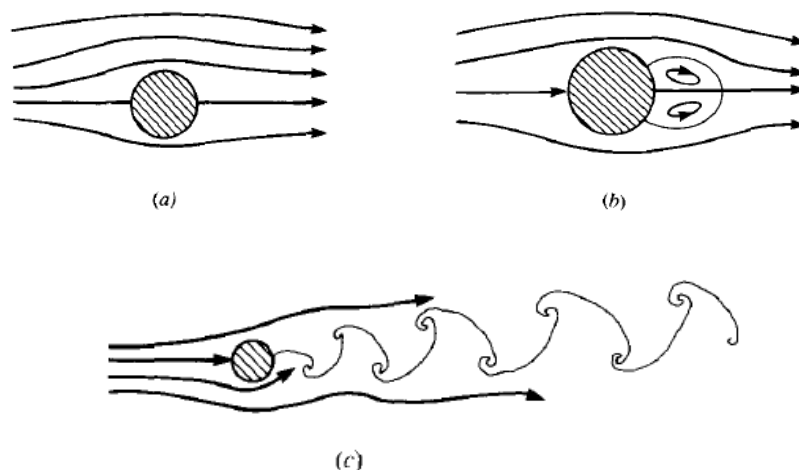


Figure 2 - Various types of flow over a circular cylinder.



For very low values of  $Re$ , approximately  $Re_d < 4$ , the flow observed (Figure 2.a) is laminar. The streamlines are almost symmetrical and the flow is attached, this regime is called Stokes flow.

When increasing the  $Re$  until approximately 40, the flow detaches on the back of the cylinder (Figure 2.b), forming two stable vortices.

As  $Re$  is increased above 40, the flow behind the cylinder becomes unstable (Figure 2.c), the vortices form now an alternately shed pattern called a Karman vortex street, named after America's best-known aerodynamicist in mid-twentieth century, the Hungarian Theodore von Karman. This pattern is exactly what we are looking for in our device, so our Reynold's number should be inside the range  $40 < Re_d < 10^5$ .

Vortex street phenomena on a stationary cylinder at Reynolds numbers up to 125 [4], shows three basic regions, a "formation region" in which the vortex street is developed and there is a large dissipation of vorticity, a "stable region" where the vortices describe a stable periodic laminar regularity, and an "unstable region" where the street disappears, turbulence is developed.

Kovaszny [5] stated that the vortices of a vortex street are not shed directly from the cylinder but develop some distance downstream ("formation region"). Taneda [6] observed that there is the possibility on the "unstable region" of a formation of a vortex street of large scale.

At much higher Reynolds numbers, on the order of  $10^5$ , the Karman vortex street will become more turbulent and it is not any more forming a regular pattern.

We will obtain the Reynolds number with the air properties and the characteristic length of the structure analysed, in our case, the diameter of the mast.

$$Re_d = \frac{\rho_{\infty} V_{\infty} D}{\mu_{\infty}} \quad (1)$$

The Reynolds calculated should be inside the desired range,  $40 < Re_d < 10^5$ .

The eddies formed transmit two forces to the structure, drag and lift. The drag is in the wind's direction and causes a torsion fixed in time, is a useless force for our purpose. However, lift sign changes alternatively, perpendicular to wind's direction, and this force is the usable one.

Humphrey [7] measured the fluctuating lift and drag on a fixed cylinder at Reynolds numbers of order  $10^5$  at the region of boundary-layer transition. The lift coefficient drops gradually as the Reynolds is increased over  $4 \cdot 10^4$  due to the increasing turbulence.

Gerrard [8] also published similar measurements at Reynolds between  $4 \cdot 10^3$  and  $10^5$ , he found that the lift coefficient was maximum at  $7 \cdot 10^4$ , being eighty times its value at Reynolds  $4 \cdot 10^3$ . However, Macovsky [9] observed that the lift coefficient diminishes for Reynolds higher than  $4 \cdot 10^4$ , when the wake is becoming turbulent and the vortex pattern three dimensional. Then, the point of maximum lift is at a lower Reynolds than the enunciated by Gerrard.

The frequency with which lift sign changes is described by Karman's formula: [1]

$$F_v = \frac{St \cdot V}{h} \quad (2)$$

Where  $F_v$  is the vortices appearance frequency,  $V$  the wind velocity,  $h$  the characteristic length, in our case the cylinder diameter, and  $St$  the dimensionless Strouhal number of the fluid.

When describing periodic fluid flows, and therefore, for wind rotating turbines design or for Vortex, the Strouhal number has a big importance.

As we have explained, flows around blunt bodies at high Reynolds numbers generate a periodic release of alternate vortices. This phenomenon is described by the Strouhal number, that defines the dimensionless frequency of this vortex shedding.

Since the end of 19th century, several values of  $St$  have been estimated for a large variety of periodic fluid phenomena. It has been proved that the approximation  $St \sim 0.16$  describes reasonably lots of them. [10]

In 1878 Strouhal [11] defined the first approximation  $St = 0.185$ . After him, Roshko [12] postulated  $St \sim 0.16$  for  $2D$  blunt boddies. For cylinders of high aspect ratio, Steinman estimated  $St \sim 0.18$  in the Reynolds range  $10^3 < Re_d < 10^5$ .

The first attempt to obtain a mathematical definition for the dimensionless number was carried out by Levi [13]. Who represented the oscillating fluid as a harmonic oscillator vibrating with a frequency according to a resonator model. That lead him to the expression:

$$St = \frac{1}{2\pi} \sim 0.16 \quad (3)$$

By unsteady numerical computations, Rosetti [14] found  $St \sim 0.24$  for smooth circular cylinders at high Reynolds.

In the case of horizontal-axis wind turbines, Medici and Alfredsson [15] measured in wind tunnel experiments  $0.12 < St < 0.20$ . And it has been observed in several experiments that  $St \sim 0.16$  is a good approximation for these cases, even though it varies with the tip speed ratio of the blades.

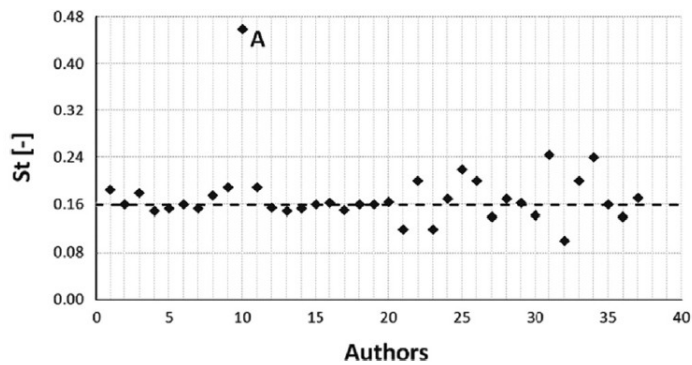


Figure 3 - Strouhal number estimations by many authors for a variety of periodic fluid flows

Lots of the estimations and measurements of the Strouhal number through decades have been plotted together on the figure above. Even though these measurements represent a variety of fluid flows, different  $2D$  and  $3D$  geometries, different Reynolds ranges, etc.; there seems to be a homogeneity around  $St \sim 0.16$ .

The reason of that is not fully understood yet, despite the existing effective models like Levi's. However, it is assumed the validity of his model,  $St \sim 0.16$ .

Another possible analysis that we could do to understand better the flow around "Vortex" is studying a similar elongated structure, like a tall building. [16]

When simulating a tall rectangular building of relative dimensions {width:length:height = 1:0.8889:4.6667}, some conclusions are obtained. Even if our device of study is much more elongated ({1:1:18}), some conceptual concepts can be better understood.

The unsteady flow field observed is quite complex, but it can be seen a turbulent vortex structure of four major vortex systems. These are:

1. The dominant unsteady large-scale structure is the Karman vortex street, with axes in the vertical direction. An oscillation of the lift produced is expected. (Figure 4)
2. The secondary currents generated by the flow separation on the roof and the large circulation cavity behind the building, having axes in the width wise direction. This roof vortex-shedding has frequency twice as large as that of Karman vortex shedding. (Figure 3-A)
3. The horseshoe vortex around the building near the ground, that induces a reverse flow at the front side. (Figure 3-B)
4. Twin axial vortices issuing from the side edges of the roof. (This structure will not be seen in our model, as it's a cylindrical structure)

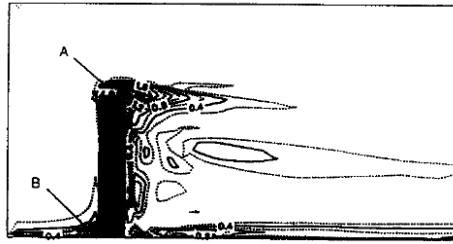


Figure 4 - Computed time-averaged vorticity contour on the symmetrical plane in a shear flow around a tall building

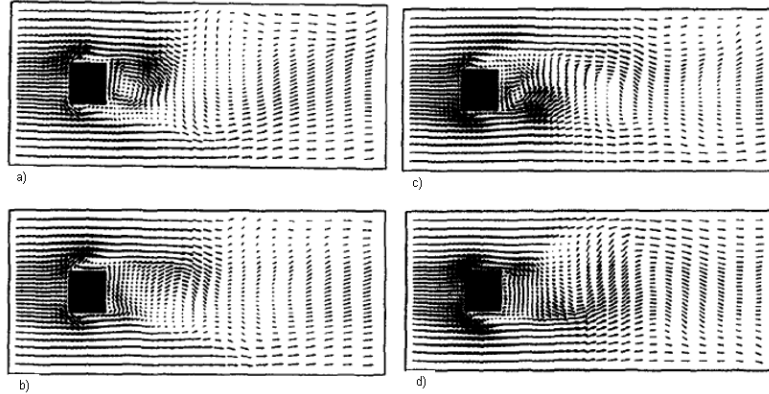


Figure 5 - Instantaneous velocity vectors in a shear flow around a tall building during vortex-shedding process

When looking for the desired Von Karman vortex generation (Figures 2.c & 4), vortex structures 2 and 3, showed on the building case, difficult this goal.

Close to the ground a reverse flow is formed and it perturbs the incident flow, that we wanted to be laminar (vortex structure 2). Besides, the roof vortex-shedding, that creates a cavity downwash the surface, disable the Von Karman vortex development. (vortex structure 3). Therefore, a high mast is recommended, to have more useful domain, and minimize these two perturbations.

The need of a high mast is reinforced by the existence of the vertical wind gradient. It is known that ground's friction slows the wind, making its speed increase with height, starting from zero, due to non-slip condition.

Various approaches for a quantitative description of the vertical wind profile have been developed. The following semi-empirical approach, called Hellmann's exponential law, is commonly used for engineering and particularly for wind turbines:

$$V_z(z) = V_h \left( \frac{z}{h_{ref}} \right)^{\alpha_{Hell}} \quad (4)$$

Where  $z$  is the height at which air speed needs to be known,  $h_{ref}$  the height at which air speed is known and  $V_z$  and  $V_h$  are the unknown and known air speeds, respectively. Finally,  $\alpha_{Hell}$  is the Hellmann-Exponent or roughness exponent.

Stability	Open water surface	Flat, open coast	Cities, villages
Unstable	0.06	0.11	0.27
Neutral	0.10	0.16	0.34
Stable	0.27	0.40	0.60

Table 2 - Approximation values for the Hellmann-Exponent depending on location and stratification stability [17]

Best fitting Hellmann-Exponent to wind turbines conditions is 0.16, corresponding to a neutral stability on flat, open coast wind conditions.

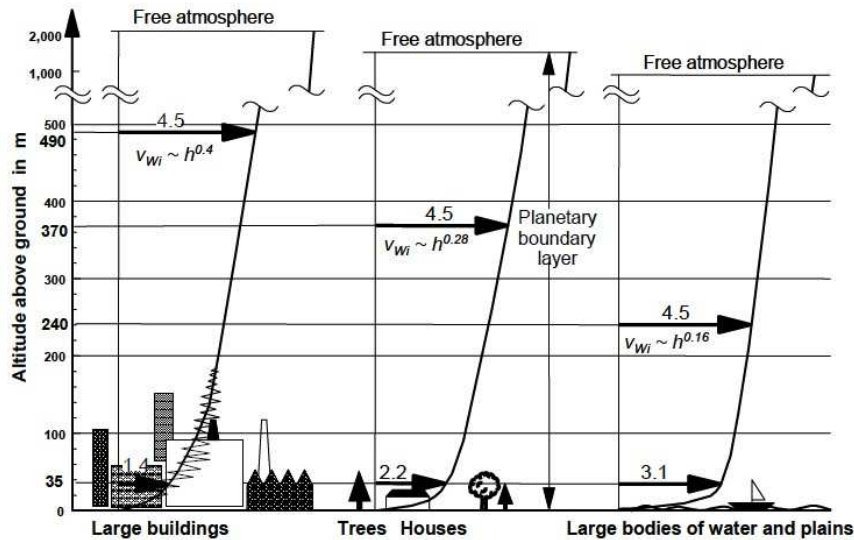


Figure 6 - Wind gradient with different Hellmann's exponents

As we can observe on Figure 6, the best topography for wind turbines is the one chosen, as it has a lower roughness and less obstacles. Even though, the velocity differences on the first 200 m are remarkable, and this domain is the one that affects wind turbines.

Because of that, it is important to consider this gradient when synchronizing lift forces along the mast for a correct operation of the device. We want the vortex generation to be simultaneous and have a unique vortex frequency along the pole.

To achieve this simultaneous effect, the section of the mast must be variable with height. With equation 2 (Karman's formula), once we have the wind velocities depending on the height ( $V_z(z)$ ) (equation 5), we set the vortex frequency we want and we can obtain the diameter of the cone as a function of height.

$$D(z) = \frac{St \cdot V_z(z)}{F_v} \quad (5)$$

On the official patent, we find the dimensions of a 4-meter height Vortex. The radius variation depending on the height is showed on the following figure:

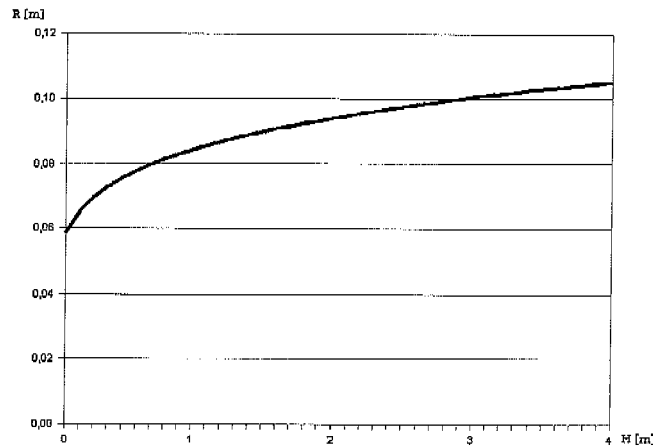


Figure 7 - Radius of the column depending on his height [1]

We have obtained the equation of radius variation depending on height using a linear regression in Excel. The equation obtained was:

$$R = 0.0012h^3 - 0.01h^2 + 0.0322h + 0.0608 \quad (6)$$

This geometry is designed for a wind governed by a Hellman's exponential coefficient of  $\alpha_{Hell} = 0.16$  and a mean air speed at 10-meter height of  $V_h = 6.5 \text{ m/s}$ , for a desired oscillation frequency of 8 Hertz. [1]

At these conditions, frequency is maintained near 8 Hz with high precision. If we calculate the frequency in the case of a constant diameter, a regular cylinder, it changes almost 2 Hz from 1 metre- to 4 metres-height.

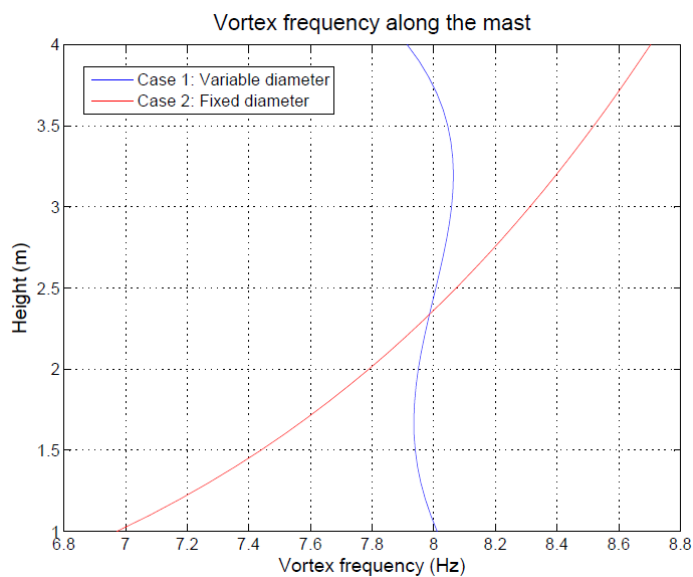


Figure 8 - Vortex generation frequencies along the mast with 1) Variable section, 2) Constant section

### 2.1.2. Vibrating structure

Once the vortices are being developed downwash the structure, an alternated lift starts the oscillation of the device. This oscillation is enhanced by two rings of magnets at the base of the moving cone.

When analysing the vortex-street wake formed downwash a vibrating circular cylinder, some changes are observed respect to a stationary cylinder case under same conditions. As the movement starts, the interaction between the body motion and the wake will cause changes in the vortex formation, strength and spacing as well as in the fluid forces the structure is submitted to.

There is a range of frequencies near the Strouhal frequency of vortex shedding ( $80 - 120\% F_v$ ) where the cylinder motion forces the vortex shedding to take place at the cylinder vibration frequency, and not at the Strouhal frequency. That is also called synchronization or wake capture. [18]

Some experiments under this “locked-in” frequency condition have showed the consequences of this phenomenon on the vortex shedding. The original flow-visualization study of a cylinder vibrating laterally with a synchronized frequency was published by Koopmann [19] for Reynolds numbers between 100 and 300. After him, Griffin [20] and Griffin & Votaw [21] studied the dependence of the vortex formation length and wake structure on the amplitude and frequency of vibration. These experiments also showed that the three regimes of the Karman street (formation, stable and unstable regions, observed on Fig. 9) are found at Reynolds numbers up to 350 for the vibrating cylinder case.

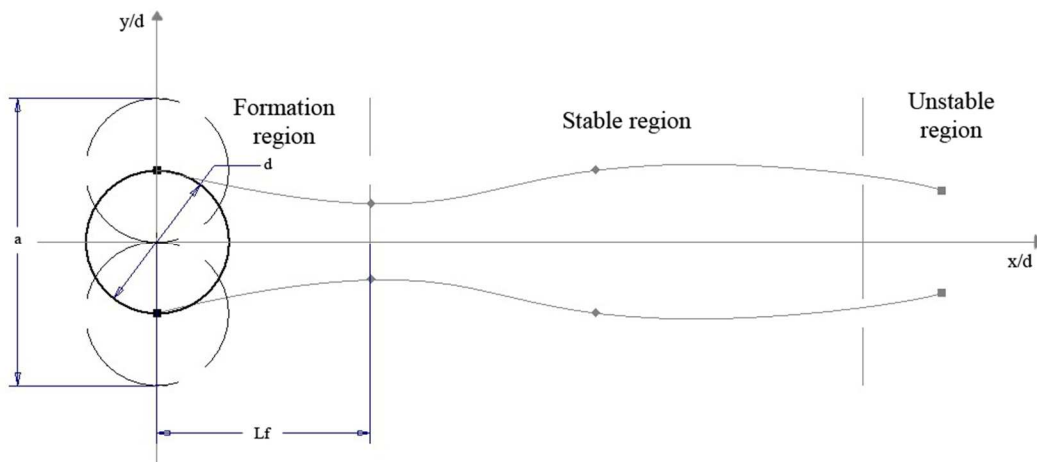


Figure 9 - Lateral vibrations of a cylinder and wake regions formed

Griffin's investigations resulted on the following relation:

$$\frac{l_F}{d} = -3.2 - 3.3 \ln St^*, St^* = St \frac{f}{F_v} \left(1 + \frac{a}{d}\right) \quad (7)$$

Where  $d_F$  is the wake width, the lateral spacing measured between the maxima of velocity fluctuations at  $x = l_F$ , the length of the formation region. The Strouhal modified parameter to characterize the lock-in phenomenon is represented by  $St^*$ . The peak to peak amplitude of the vibration is represented by  $a$  and the diameter of the cylinder is defined as  $d$ .

Some observations were made:

- The length of the formation region ( $l_F$ ) decreases systematically with increased amplitude of vibration ( $a$ ).
- When the vibration frequency ( $f$ ) is less than the Strouhal frequency ( $F_v$ ), the length of the formation region is increased, and in the opposite case, the formation region is reduced.
- The lateral spacing ( $d_F$ ) decreases with the amplitude of vibration and increases with frequency.

On experiments was observed too that vortex strength or circulation is much higher than in the stationary case (an increase of 65% was achieved), and increases with the amplitude of vibration. Concerning to the rate of vorticity generation, it increases 50% at an amplitude of  $0,3d$  and by 70% at  $0,48d$  compared to a stationary cylinder wake. [4]

All those changes on the vortex street result on changes on the fluid forces too. With the body oscillations, an increasing of the lift on the surface of the structure is produced. Bishop & Hassan [22] found that the lift coefficient on a cylinder vibrating at  $a/d = 0.5$  was double the stationary cylinder value for  $f/F_v = 0.95$  and  $Re = 6000$ . A higher drag is also observed.

Opposite to the lift reduction in a fixed cylinder observed above Reynolds numbers of  $10^6$ , Den Hartog [18] remarked that large industrial smokestacks vibrate violently at the "correct" Strouhal frequency at Reynolds numbers as high as  $7 \cdot 10^6$ .

All that said, our objective will be then make the structure vibrate at a frequency nearby the Strouhal one ( $F_v$ ), to increase the vortex strength and the lift force over the mast.



## 2.2. Resonance

Resonance is a physical phenomenon that occurs on a rigid body when the frequency of the excitation force on the system becomes equal to the system's natural frequency ( $f_n$ ).

When resonance occurs in an undamped system, the amplitude (or displacement) of the vibration of the body grows without bound, to infinity, as we observe in Fig. 10.

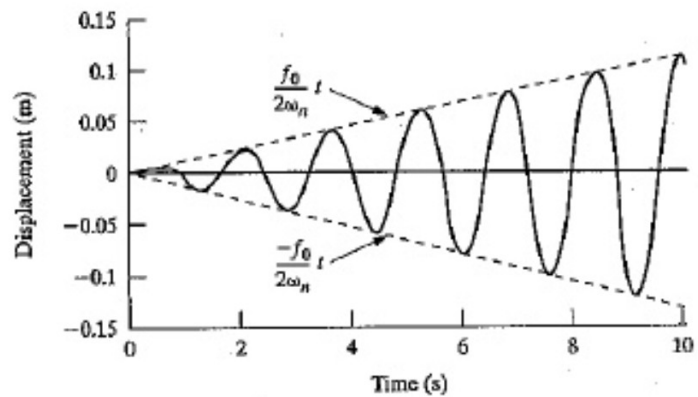


Figure 10 - Forced response of a spring-mass system driven harmonically at its natural frequency, called resonance[23]

In the case of a damped system, not ideal, the amplitude of the vibration increase deeply but this increase is reduced as the damping ratio ( $\xi$ ) gets bigger.

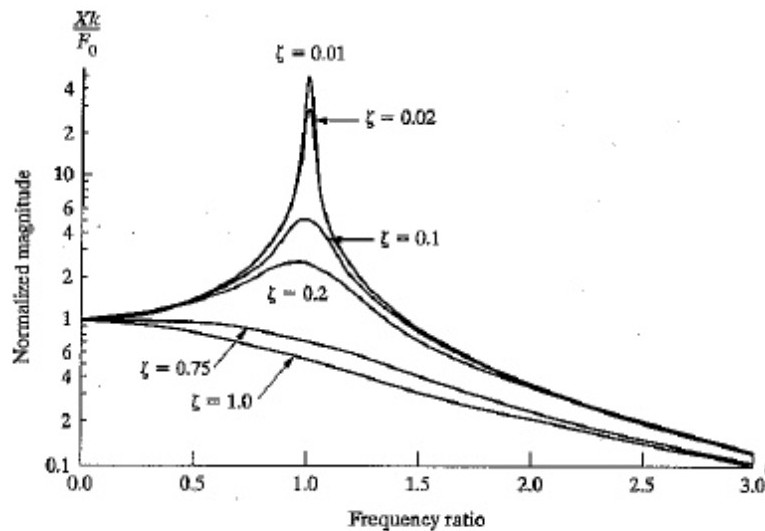


Figure 11 - Magnitude of the steady-state response versus the frequency ratio for several values of the damping ratio ( $\xi$ ) [23]

The structure of "Vortex" has several spatial oscillatory modes. As a mast anchored from one end, the first oscillation mode is that in which one end is static and the other has maximum amplitude, the tip of the pole. Then, its natural oscillation frequency for the  $n$ th harmonic is given by:

$$f_n = \frac{1}{2\pi} \sqrt{\frac{IE}{d_1} K_n^4 - a^2} \quad (8)$$

Where  $I$  is the sectional moment of inertia,  $E$  is the Young's modulus of the material,  $d_l$  is the density of the bar per unit length,  $K_n$  is the  $n$ th oscillation mode and  $a$  the damping constant. [1]

If the natural oscillation frequency of the mast ( $f_n$ ) is equal, or close, to the vortex shedding frequency ( $F_v$ ) (equation 2), self-excited resonant vibrations can occur on the structure if the damping of the system is sufficiently low, maximizing the capacity of aeroelastic energy absorption. This phenomenon, so avoided in certain structures as bridges or tall buildings, is the desired goal of our device.

When resonance occurs, a dynamic aeroelastic phenomenon called "*flutter*" could happen. It is an instability that generally leads to a catastrophic structural failure (e.g. Tacoma Narrows Bridge).

An elastic structure under an aerodynamic load starts vibrating, self-induced by Karman vortices, the load is reduced when the structure deflects, as the load is reduced the deflexion is reduced too, the initial load is restored and this cycle gets repeated. The amplitude gets bigger and bigger with this resonance and could cause structural failure. [24]

Because of this, structures exposed to aerodynamic forces, as wings, airfoils, chimneys, bridges, etc., are carefully designed to avoid "*flutter*". However, in our case of study this phenomenon is our goal to maximize the oscillation of the pole and therefore maximize the generation of electrical energy of the wind turbine.

## 2.3. Electromechanical coupling

The structure of “Vortex” uses materials with high electromechanical coupling to convert the aeroelastic energy absorbed into electrical energy.

This effect is exhibited by certain materials in which when a force is applied between two of their faces, a potential difference is created between them. Its operation is reversible, the presence of a voltage between two faces causes a deformation.

These materials are commonly used as actuators, speakers, sensors, etc. They are also applied, but is not so usual, for electrical energy generation. For example, floors that transform the energy of pedestrian’s steps, clothes, footwear or electric lighters that obtain usable electrical energy from movement.

The efficiency of these materials in the energy transformation process is highly variable and it is difficult to find materials with efficiency greater than 75%, as there is always an amount of energy that is transformed into elastic potential energy. In the resonance case, a substantial part of this energy is recovered and an efficiency close to 100% is achieved, optimising the energy transformation on “Vortex”.

Another purpose of the use of these materials is related to the need of making the natural frequency of oscillation of the structure ( $f_n$ ) equal to the vortex formation frequency ( $F_v$ ).

The vortex frequency cannot be modified, but it is possible to modify any of the control parameters on which the natural frequency depends (equation 8). Of all parameters, the easiest one to modify is the Young’s modulus. Thanks to the electromechanical coupling, modulating the voltage to which are subjected the materials, using an electronic control unit, we could make both frequencies be equal.

Wind’s velocity can be obtained using the stationary torsion of the mast generated by the drag force. [1]

The use of materials with high electromechanical coupling closes then the transformation of wind’s energy into usable electrical energy.

## 3. Computational Analysis

After the theoretical analysis, we could simulate the behaviour of the structure under the air forces with CFD, but we would only see the initial generation of vortices and the initial forces.

To see the interaction of the fluid forces effect and the structure response, we could an FSI simulation. The Fluid Structure Interaction is an option of Fluent, an Ansys software, with which we would be able to see the stress and strain of the structure caused by the fluid forces on it. With this software, we could do a dynamic analysis to see the changes on the vortex street and the fluid forces caused by the vibration of the structure, as well as the stresses on it.

As fluid-structure interaction problems are complex to simulate and are still a challenge, we won't perform a computational analysis but we will introduce the software basis.

### 3.1. FSI software

Several numerical methods for computing fluid-structure interaction (FSI) problems have been developed the last few decades.

They have several scientific and engineering applications, as they allow the simultaneous calculation of stresses on a solid structure produced by the aerodynamical load of an internal or surrounding flow.

Analytical solutions are impossible for most of those problems, and the experimental method is also limited, therefore numerical resolutions are the best option; especially thanks to the improvements of computational powers.

Even though, FSI problems are still a challenge due to their strong nonlinearity and multidisciplinary nature; besides all the difficulties of fluid simulation, obtaining a good coupling between structure and fluid calculations is not easy.

The numerical procedures to solve FSI problems are classified into two approaches: monolithic approach and partitioned approach.

- The monolithic approach treats the fluid and structure dynamics as one computational field, they form a single system equation, which is solved by a unified algorithm. The interfacial conditions are implicit in the procedure. This approach could achieve a better accuracy in a multidisciplinary problem, but it requires more resources and the code is very complex.
- With the partitioned approach, instead, the fluid dynamics and the structural mechanics are solved separately. Divided as two different computational fields, each one is solved with its respective mesh discretization and algorithm. The interfacial conditions in this case are used as nexus, to coordinate information between both solutions; as their location is not known and variable, this could be a source of error. This approach is very powerful, however, it's hard to coordinate both solutions and obtain an accurate result.

Another possible classification is based on the mesh adopted, there are conforming mesh methods and non-conforming mesh methods; we can observe the differences in Fig. 12.

- A conforming mesh method considers the interface as a physical boundary, so, it treats the interface location as part of the solution. It requires re-meshing when a deformation or movement of the solid structure is produced. The iterative process would be: solve the fluid field assuming an initial interface location, apply the obtained fluid pressure and stress as external forces, update the position and/or deformation of the structure and re-mesh the fluid domain. The main difficulty of this method is to maintain proper data transfer between the disciplines to obtain a converged solution with efficiency and accuracy. The data transfer on the interface is degraded by the gaps and discontinuities on the junction of both meshes. The fluid mesh is refined at the proximities of the interface, while the structural mesh refinement will be around the high stress areas which most likely will not be on the interface.
- In contrast, a non-conforming mesh method treat the boundary location and the interface conditions as constraints imposed. Then, re-meshing is not necessary, and the fluid and solids equations can be solved separately.

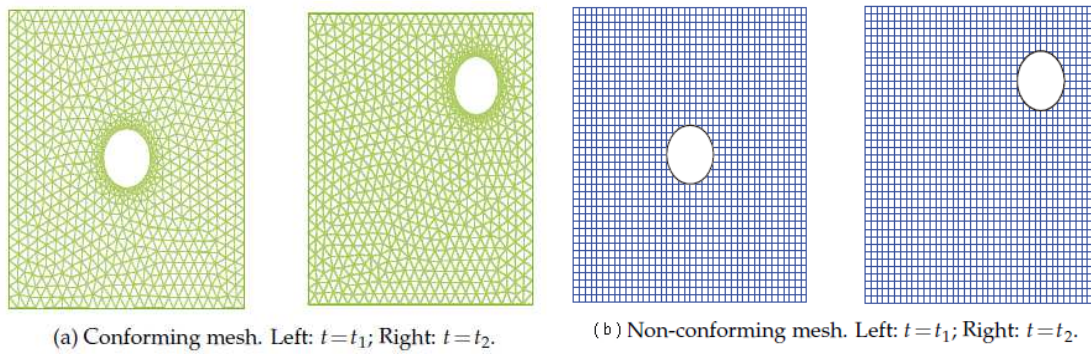


Figure 12 - Examples of conforming mesh (a) and non-conforming mesh (b)

When using the partitioned approach most problems require a conforming mesh method, whereas the immersed methods use a non-conforming mesh.

The methods presented are interesting for our case of study, the behaviour and stresses of an hyperelastic structure under wind loads could be analysed.

The software ANSYS includes already FSI applications which then we could calculate simultaneously the aerodynamic forces on the structure and the velocity that the deformed structure imparts to the fluid.

This interaction is especially important in our model, as we want the structure to reach resonance with the frequency of the Von Karman vortices of the wind. The vibration of our structure will affect a lot on the fluid flow, the movement will increase the desired behaviour, reinforcing itself.

## Conclusions

Some observations about the invention can be done after studying the whole energy transformation process.

As we have explained, the device is based on three coordinated physical principles: generation of vortices in fluids, resonance and the electromechanical coupling of some material. These principles have never been before used together for generating electric energy.

In the aerodynamical field, no wind turbine has been found which intentionally seeks to synchronise the appearance of the turbulent vortices generated in its geometry. "Vortex" has into account the wind gradient and its geometry is designed for this purpose.

Focusing on the resonance, no electric generator before has looked for resonance, tuning the natural oscillation frequency to the generation frequency of vortices. As we have observed, resonance is a powerful tool to maximize energy absorption. Historically has been avoided because of its destructive capacity on structures exposed to aerodynamic forces, but this energy could be also useful, as we have observed.

In the case of the third principle, no electrical generator based on materials with electromechanical coupling has been designed that uses the energy contained in a stationary laminar flow.

Because all these reasons, the invention of discuss has changed the traditional model of wind turbine design, and it has expanded the common applications of the stated principles.

## References

- [1] D. J. Yáñez Villarreal, "Vortex Resonance Wind Turbine," European Patent EP2602483A1, 2013.
- [2] D. Suriol, D. Yáñez, and R. Martín, "Vortex Bladeless," 2015. [Online]. Available: <http://www.vortexbladeless.com/>.
- [3] J. Anderson Jr, *Fundamentals of Aerodynamics*, vol. Third Edit. 1985.
- [4] O. M. Griffin and S. E. Ramberg, "The vortex-street wakes of vibrating cylinders," *J. Fluid Mech.*, vol. 66, no. 3, p. 553, 1974.
- [5] L. S. G. Kovaszny, "Hot-Wire Investigation of the Wake behind Cylinders at Low Reynolds Numbers," *Proc. R. Soc. A Math. Phys. Eng. Sci.*, vol. 198, no. 1053, pp. 174–190, 1949.
- [6] S. Taneda, "Studies on wake vortices (II), experimental investigation of the wake behind cylinders and plates at low Reynolds numbers," *Res. Inst. Appl. Mech.*, vol. 1, pp. 29–40, 1952.
- [7] J. S. Humphreys, "On a Circular Cylinder in a Steady Wind at Transition Reynolds Numbers," *J. Fluid Mech.*, vol. 9, p. 603, 1960.
- [8] J. H. Gerrard, "An Experimental Investigation of the Oscillating Lift and Drag of a Circular Cylinder Shedding Turbulent Vortices," *J. Fluid Mech.*, vol. 11, p. 244, 1961.
- [9] M. S. Macovsky, "Vortex Induced Vibration Studies," 1958.
- [10] F. Trivellato and M. Raciti Castelli, "Appraisal of Strouhal number in wind turbine engineering," *Renew. Sustain. Energy Rev.*, vol. 49, pp. 795–804, 2015.
- [11] C. Freese, "Vibrations of vertical pressure vessels," *J. Eng. Ind.*, pp. 77–91, 1959.
- [12] A. Roshko, "On the drag and shedding frequency of two-dimensional blunt bodies," Washington DC, 1954.
- [13] E. Levi, "A universal Strouhal law," *J Eng Mech*, pp. 718–727, 1983.
- [14] G. Rosetti, G. Vax, and A. Fajarra, "URANS calculations for smooth circular cylinder flow in a wide range of Reynolds numbers: solution verification and validation," *J. Fluids Eng.*, vol. 134, pp. 1–18.
- [15] D. Medici and P. Alfredsson, "Measurements on a wind turbine wake: 3D effects and blunt body vortex shedding," *Wind Energy 2006*, vol. 9, pp. 219–236, 2006.
- [16] C. C. S. Song and J. He, "Computation of wind flow around a tall building and the large-scale vortex structure," *J. Wind Eng. Ind. Aerodyn.*, vol. 46–47, no. C, pp. 219–228, 1993.
- [17] A. W. Martin Kaltschmitt, Wolfgang Streicher, *Renewable Energy: Technology, Economics, and Environment*. Springer, 2007.



- [18] J. P. den Hartog, "Proceedings, National Academy of Science," *J. Basic Eng.*, vol. 40, pp. 115–157, 1954.
- [19] G. H. Koopmann, "The vortex wakes of vibrating cylinders at low Reynolds numbers," *J. Fluid Mech.*, vol. 28, pp. 501–512, 1967.
- [20] O. M. Griffin, "Trans. A.S.M.E.," *J. Appl. Mech.*, vol. 38, pp. 729–738, 1971.
- [21] O. M. Griffin and C. W. Votaw, "The Vortex Street in the Wake of a Vibrating Cylinder," *J. Fluid Mech.*, vol. 55, pp. 31–48, 1972.
- [22] R. E. D. Bishop and A. Y. Hassan, "The Lift and Drag Forces on a Circular Cylinder Oscillating in a Flowing Fluid," *Proc. Roy. Soc.*, vol. 277, pp. 51–57, 1964.
- [23] D. J. Inman, *Engineering Vibration*. Prentice-Hall, 2001.
- [24] D. H. Hodges and G. A. Pierce, *Introduction to Structural Dynamics and Aeroelasticity*. 2002.